MEDICAL SCIENCE MONITOR

CLINICAL RESEARCH

e-ISSN 1643-3750
© Med Sci Monit, 2018; 24: 6861-6872
DOI: 10.12659/MSM.910388

Received: 2018.04.03
Accepted: 2018.05.30
Published: 2018.09.28

Correlation of T Cell Immunoglobulin and ITIM Domain (TIGIT) and Programmed Death 1 (PD-1) with Clinicopathological Characteristics of Renal Cell Carcinoma May Indicate Potential Targets for Treatment

Authors' Contribution:
Study Design A
Data Collection B
Statistical Analysis C
Data Interpretation D
Manuscript Preparation E
Literature Search F
Funds Collection G

ABCDEF 1,2 Xin Hong
BCD 2 Xiaofeng Wang
BCD 2 Tian Wang
AF 1 Xu Zhang

1 Department of Urology, Chinese PLA General Hospital, Beijing, P.R. China
2 Department of Urology, Peking University International Hospital, Beijing, P.R. China

Corresponding Author: Xu Zhang, e-mail: zhangxu_pla@163.com
Source of support: Departmental sources

Background: This study investigated the correlation of programmed death 1 (PD-1) and T cell immunoglobulin and ITIM domain (TIGIT) with clinicopathological characteristics of renal cell carcinoma (RCC) and explored the biological roles of both proteins in the development, metastasis, and invasion of RCC.

Material/Methods: The expressions of PD-1 and TIGIT were detected in the RCC and adjacent normal tissues, and their correlation with the clinicopathological characteristics of RCC, relationship between PD-1 and TIGIT in RCC, and the correlation of PD-1 and TIGIT expression with distance of adjacent normal tissues to RCC were further evaluated.

Results: TIGIT and PD-1 expression was detectable in the immune cells of peripheral blood mononuclear cells and lymphoid tumor infiltrating lymphocytes, and TIGIT expression was significantly higher than PD-1 expression in the same sample. Cells with transparent cytoplasm were diffuse, and several cells showed dark nuclear staining with mild atypia; the interstitium was rich in blood vessels and had mild fibrous hyperplasia, and immunofluorescence staining showed cells were positive for TIGIT. The expression of PD-1 and TIGIT was significantly different between RCC and adjacent normal tissues ($P<0.05$). Positive PD-1 expression was closely related to tumor size and Fuhrman grade ($P<0.05$). The expression of TIGIT and PD-1 was related to the distance of adjacent normal tissues to RCC ($P<0.05$).

Conclusions: The activation of PD-1 and TIGIT may exert negative regulatory effects and inhibit the immune response to cancer cells, resulting in immune escape of cancer cells. Both PD-1 and TIGIT may serve as potential targets for the treatment of RCC.

MeSH Keywords: Apoptosis • Carcinoma, Renal Cell • Immunoglobulin Allotypes

Full-text PDF: https://www.medscimonit.com/abstract/index/idArt/910388

3677 7 6 22

Indexed in: [Current Contents/Clinical Medicine] [SCI Expanded] [ISI Alerting System] [ISI Journals Master List] [Index Medicus/MEDLINE] [EMBASE/Excerpta Medica] [Chemical Abstracts/CAS]

Background

Renal cell carcinoma (RCC) is a malignancy that originates in the epithelial system of the urinary tract in renal parenchyma and accounts for 80–90% of renal malignancies. Clear cell RCC (ccRCC) is the main pathological type of RCC and accounts for about 85% of RCC [1]. RCC is the third most common malignancy of the urinary system [2], and the 5-year survival rate of RCC patients is only 12.1%. It has been reported that 342 501 patients were diagnosed with RCC between 2001 and 2010 in the USA and its incidence is still increasing [3,4]. Surgery is still an effective treatment for RCC, but 20–30% of RCC patients develop recurrence within 3 years [5,6]. The lungs are the most common site of metastasis of RCC [7]. Moreover, RCC is generally insensitive to traditional chemotherapeutics, and patients with advanced RCC usually have an extremely poor prognosis.

Immune therapy uses the immune system to defend against cancer. It has become a focus in the field of cancer treatment. In 2013, immune therapy was acclaimed at the foremost scientific breakthrough by the journal Science [8].

Programmed death 1 (PD-1) belongs to the CD28/CTLA-4 family. It is a type I transmembrane glycoprotein composed of 288 amino acids and belongs to the immunoglobulin superfamily. PD-1 is expressed on T cells, B cells, natural killer cells, monocytes, and dendritic cells (DC) [9]. PD-1 can bind to its ligand PD-L1 to inhibit T cell-mediated cellular immunity. Thus, the activation of PD-1/PD-L1 in cancer may exert negative regulatory effects and inhibit the immune response to cancer cells, which is an important mechanism underlying the immune escape of cancer cells [10].

T cell immunoglobulin and ITIM domain (TIGIT) is a new immune molecule identified in recent years; it has an immunoglobulin-like domain, a transmembrane region, and an immunoreceptor protein tyrosine inhibitory motif (ITIM) (Figure 1) [11]. TIGIT belongs to the poliovirus receptor (PVR)/desmin family and a subgroup of the immunoglobulin superfamily. TIGIT and its ligand are highly expressed in some cancers, including colorectal cancer, gastric cancer, and neuroblastoma [12], and are involved in the tumor immune cycle at different levels. However, no study has reported the role of TIGIT in human RCC.

In the present study, 60 patients with ccRCC were recruited. The tumor infiltrating lymphocytes (TIL) were detected, and then biotin-streptavidin analysis and flow cytometry were used to detect NK cells, NKT, CD4+ T cells, and CD8+ T cells in the ccRCC. Finally, immunohistochemistry was done with Elivision method to detect the PD-1 and TIGIT expression in the ccRCC and adjacent normal tissues. This study investigated the correlation of PD-1 and TIGIT expression with the clinicopathological characteristics of ccRCC (such as grade, stage, and metastasis) and with the distance of adjacent normal tissues to ccRCC (0.5 cm, 1.0 cm, and 2.0 cm). These findings may inform the clinical diagnosis, extent of surgical resection, prognosis determination, and target therapy of ccRCC patients.

Material and Methods

Sample collection

This study was approved by the Ethics Committee of the Chinese PLA General Hospital (2015-I-1). ccRCC tissues (n=60) were collected from patients who received radical surgery for RCC and were pathologically diagnosed with ccRCC after surgery between June 2015 and July 2017. The adjacent normal tissues were also harvested and confirmed to have no invasion of cancer cells. In addition, normal renal tissues were collected from 5 patients without malignancies (kidney trauma or kidney stones). The medical histories were complete. Patients did not receive radiotherapy, chemotherapy, or biological therapy before surgery. Post-operative pathology and imaging examination were used to determine the clinical stage and metastasis. HE staining was done in renal tissues for further validation of clinical staging.

In 60 patients with ccRCC, there were 38 males and 22 females. The median age was 55.6 years (range: 25–76 years). In addition, 26 patients were no older than 50 years and 34 were older than 50 years. The median tumor diameter was 4.7 cm (range: 1.2–13.0 cm). Moreover, the tumor diameter was ≤4.0 cm in 27 patients and >4.0 cm in 33 patients. According to the Fuhrman grading system (WHO, 1997), high differentiation was noted in 45 cases, intermediate differentiation in 10, and poor differentiation in 5. According to the AJCC clinical staging system (2010), stage I ccRCC was found in 40 cases, stage II in 16, and stage III in 4 (Table 1).

Immunofluorescence staining

The ccRCC tissues and adjacent normal tissues were collected, embedded in paraffin, and sectioned (4-μm). Sections were heated at 70°C for 2 h and the allowed to cool to room temperature. Then, sections were deparaffinized in xylene for 3 min and degreased in 100%, 95%, 85%, and 75% ethanol (3 min for each). The sections were washed in flowing water and then in PBS 3 times (2 min each). After antigen retrieval in citric acid buffer for 10 min in a microwave oven, the sections were allowed to cool to room temperature within 1–2 h. After washing in PBS 3 times (2 min each), sections were treated with 3% hydrogen peroxide to inactivate endogenous peroxidase in the dark at room temperature for 15 min. After washing in PBS 3 times (2 min each), sections were incubated with primary antibody at 4°C overnight and then in secondary antibody for 1 h, followed by DAB staining.

Indexed in: [Current Contents/Clinical Medicine] [SCI Expanded] [ISI Alerting System] [ISI Journals Master List] [Index Medicus/MEDLINE] [EMBASE/Excerpta Medica] [Chemical Abstracts/CAS]

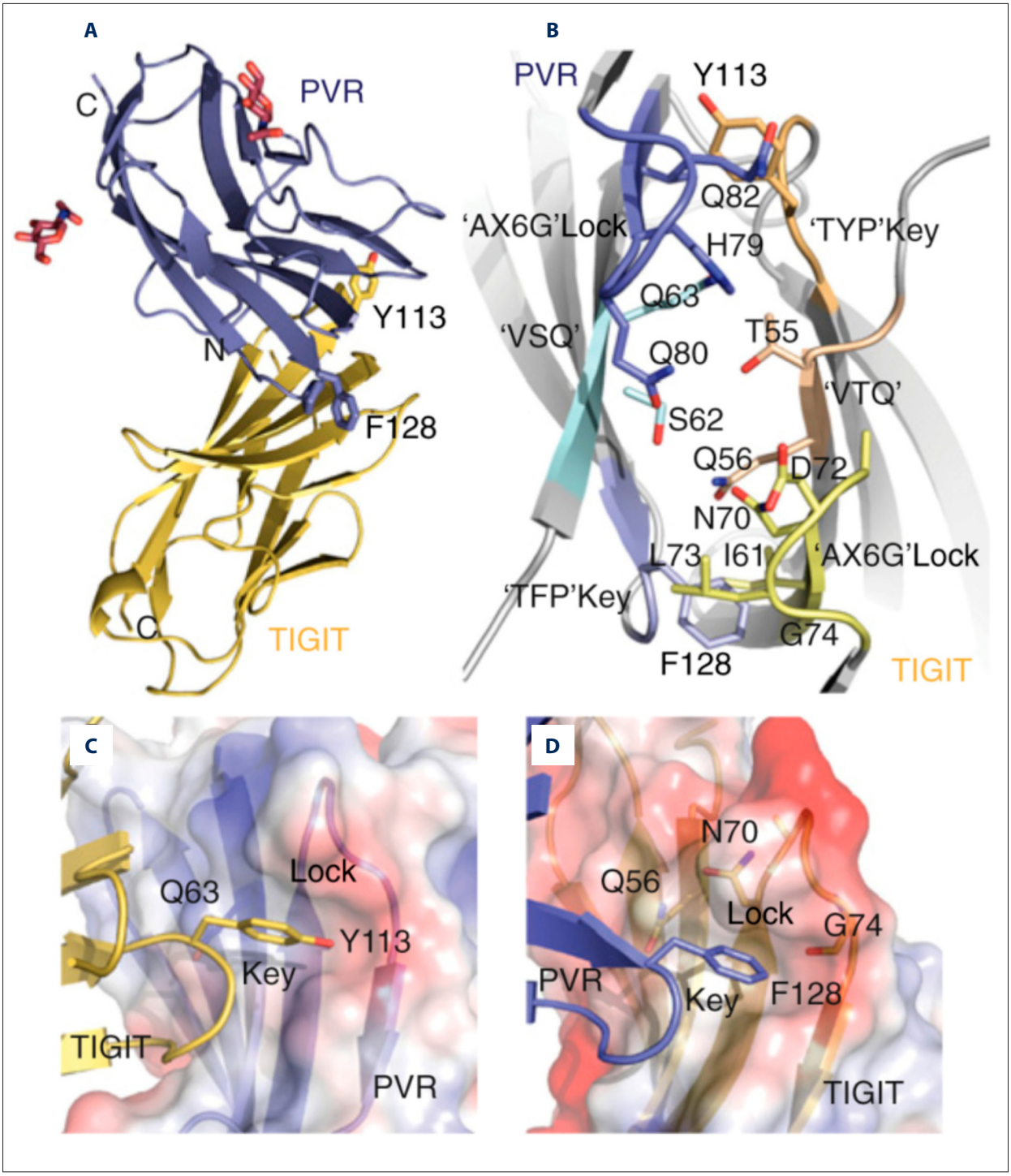

Figure 1. Structure of TIGIT-PVR complex. TIGIT contains immunoglobulin-like domain, transmembrane region, and immunoreceptor protein tyrosine inhibitory motif; it is polyomavirus receptor/desmin and is a subgroup of the immunoglobulin superfamily. (**A**) TIGIT IgV domain (gold) in the complex with PVR D1 domain (blue) and sugar moieties (red). The TIGIT/PVR interface shows a conserved lock-and-key (**B**) interaction between 2 molecules. The "lock" is formed by the AX6G motif, and the "key" is formed by the corresponding T(Y/F)P motif on the neighboring molecule. The "key" residues Tyr113 and Phe128 in the conserved TIGIT motif TYP and the PVR motif TFP are labeled. Both (V/I) and (S/T)Q motifs also locate in the complex interface. (**C**) The "key" formed by Tyr113 in TIGIT and the lock formed by the AX6G motif of PVR. (**D**) The "key" formed by Phe128 on PVR and the lock formed by the AX6G motif of TIGIT.

Indexed in: [Current Contents/Clinical Medicine] [SCI Expanded] [ISI Alerting System] [ISI Journals Master List] [Index Medicus/MEDLINE] [EMBASE/Excerpta Medica] [Chemical Abstracts/CAS]

Table 1. Clinical characteristics of 60 patients with ccRCC.

Variable	n	Proportion (%)
Age (year)		
≤50	26	43.3
>50	34	56.7
Sex		
Male	38	63.3
Female	22	36.7
Tumor diameter (cm)		
≤4.0	27	45.0
>4.0	33	55.0
Fuhrman grade		
Well differentiated	45	75.0
Intermediately differentiated	10	16.7
Poorly differentiated	5	8.3
TNM stage		
Stage I	40	66.7
Stage II	16	26.7
Stage III	4	6.6
Stage IV	0	0.0

PAS staining: sections were treated with periodic acid for 10 min, Schiff solution for 15–30 min in the dark, and hematoxylin for nuclear staining. After dehydration and transparentizing, sections were mounted with neutral resin.

Flow cytometry

ccRCC tissues and peripheral blood were collected from ccRCC patients. Myeloid cells and TILs were collected from cancer tissues. The cancer tissues were ground and digested with collagenase, and then cells were re-suspended in PBS. After filtration through a 70-μm mesh, PBS was added to the filtrate until the volume was 30 ml. Then, the filtrate was added into a 50-ml centrifuge tube containing 15-ml lymphocyte separation fluid, followed by density gradient centrifugation for 20 min. The middle white blood cell layer was carefully collected and transferred into a tube containing PBS, followed by centrifugation. The supernatant was removed and TILs were harvested. Cells were re-suspended in PBS and counted. The peripheral blood underwent the same procedures for the collection of PBMC. Cells were subjected to Fixable Viability Dye eFluor 506 staining. Cells were washed 20 min later and surface molecules were stained for 20 min according to the following procedures: after staining, cells were washed, and then re-suspended in FACS buffer, followed by flow cytometry (Fortessa). The cells were detected as much as possible. Analysis of data was done with FlowJo software.

Immunohistochemistry with Elivision method

Sections were deparaffinized twice in xylene (10 min each) and then rehydrated in 100% ethanol for 2 min, 95% ethanol for 2 min, 80% ethanol for 2 min, 70% ethanol for 2 min, tap water for 5 min, and distilled water for 5 min. Then, sections were treated with 30% H_2O_2 for 10 min at room temperature to block endogenous peroxidases. After washing in distilled water for 5 min and in PBS for 5 min, antigen retrieval was done in a microwave oven twice (5 min for each). Then, the sections were allowed to cool to room temperature within 20 min and subsequently treated with 10% normal goat serum in PBS for 1 h at 37°C. Sections were incubated with primary antibody (anti-human TIGIT/VSTM3 antibody) in PBS overnight at 4°C. After washing 3 times with PBS (5 min each), sections were incubated with HRP-conjugated secondary antibody (goat anti-rabbit IgG) in PBS for 30 min at 37°C. After washing in PBS 3 times (3 min for each), visualization was done with DAB, and then the sections were gently rinsed with tap water for about 1–2 min. Counterstaining was done with hematoxylin, followed by incubation twice with 100% ethanol (2 min each) and xylene twice (5 min each). Sections were finally mounted with neutral resin. The staining was evaluated by 2 experienced pathologists in a blind manner and any discrepancies were resolved by negotiation. To determine the number of positive cells, sections were first observed at low magnification. Then, at high magnification (×400), positive cells were counted in 5 randomly selected fields, and a mean was calculated. The mean number of positive cells was determined in 60 patients, and expression levels were classified as strongly positive (+++), positive (++), weakly positive (+), and negative (–) according to the number of positive cells.

Statistical analysis

Statistical analysis was performed with SPSS version 20.0 for Windows and the chi-square test was used for comparison, depending on the distribution of data. The correlation between PD-1 expression and TIGIT expression in ccRCC was evaluated with Spearman rank correlation analysis. The correlation of PD-1 and TIGIT expression with distance of adjacent normal tissues to ccRCC (0.5, 1.0, and 2.0 cm) was evaluated with the Kruskal-Wallis H test. Paired comparisons were done with the Wilcoxon rank sum test. A value of $P<0.05$ was considered statistically significant with α at 0.05.

Indexed in: [Current Contents/Clinical Medicine] [SCI Expanded] [ISI Alerting System] [ISI Journals Master List] [Index Medicus/MEDLINE] [EMBASE/Excerpta Medica] [Chemical Abstracts/CAS]

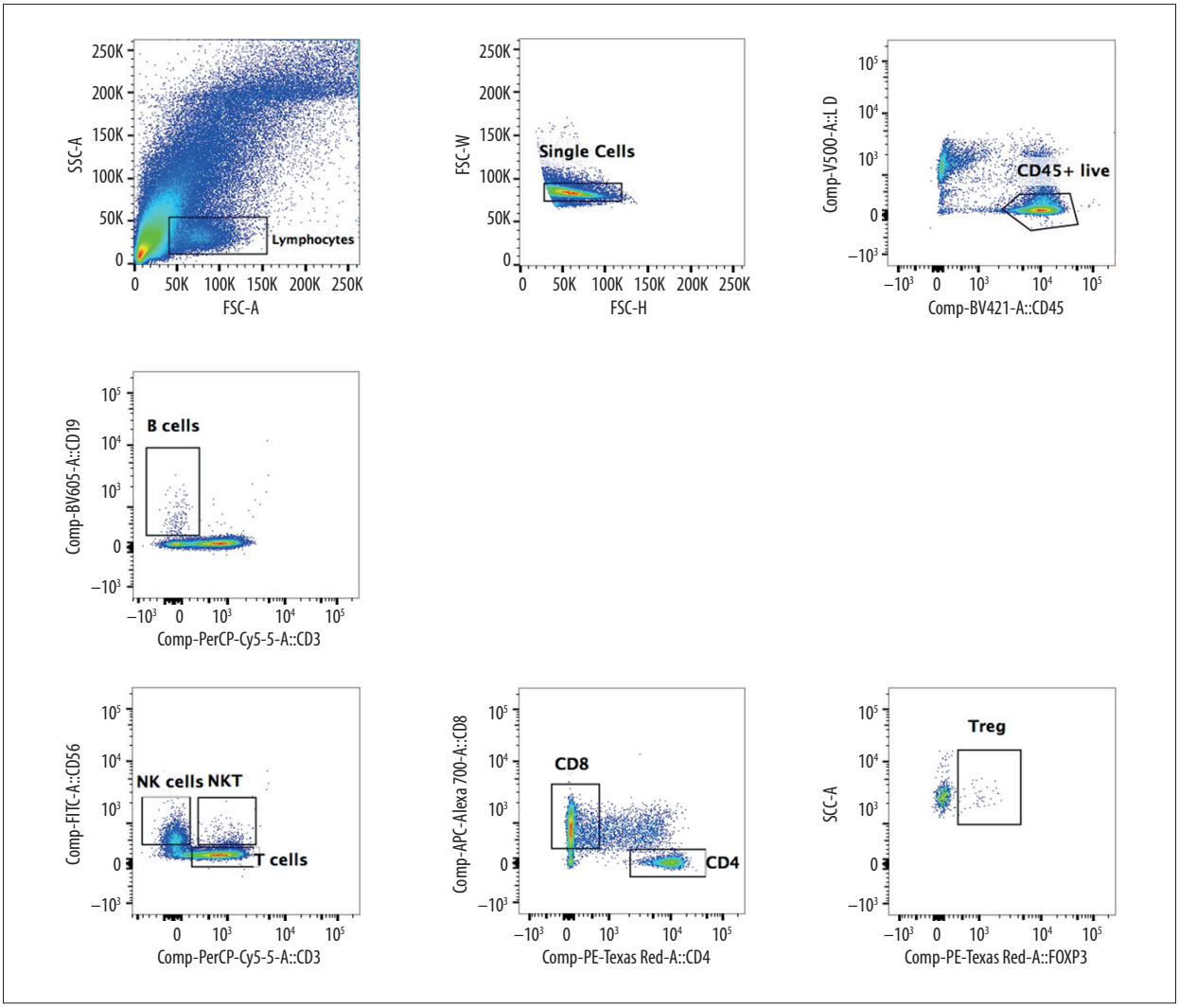

Figure 2. Flow cytometry of lymphocytes in ccRCC. The TILs were separated from ccRCC, including B cells, T cells (CD4+T cells and CD8+T cells), NK cells, NKT cells, and Treg cells. The proportion of TILs increased significantly, especially the proportion of CD8+T cells.

Results

TIGIT and PD-1 expression

The TILs were successfully separated from ccRCC tissues and included B cells, T cells (CD4+T cells and CD8+T cells), NK cells, NKT cells, and Treg cells (Figure 2). In the lymphoid TILs and PBMCs, TIGIT expression was detected (Figure 3) and compared with the PD-1 expression in TILs and PBMCs (Figure 4). Results showed TIGIT expression was significantly higher than PD-1 expression in the same sample.

Pathological results

The cancer tissues were subjected to pathological examination after HE staining (Figure 5). Under a light microscope, cells with transparent cytoplasm were diffuse with clear boundary, the small and round nucleus was localized at the center of a cell, few cells displayed atypia, and several cells showed dark staining with mild atypia. The interstitium was rich in blood vessels with mild fibrous hyperplasia. Immunofluorescence staining was also performed and indicated positive TIGIT expression (Figure 6).

PD-1 expression in ccRCC and adjacent normal tissues

PD-1 expression was mainly found in interstitial lymphocytes; the majority of PD-1 expression was noted in the cytoplasm, and several cells showed PD-1 expression on the cell membrane. In 60 ccRCC tissues, positive PD-1 expression was found in 22 tissues, with a positive rate of 36.7% (22/60). In adjacent normal tissues, positive PD-1 expression was noted

Indexed in: [Current Contents/Clinical Medicine] [SCI Expanded] [ISI Alerting System] [ISI Journals Master List] [Index Medicus/MEDLINE] [EMBASE/Excerpta Medica] [Chemical Abstracts/CAS]

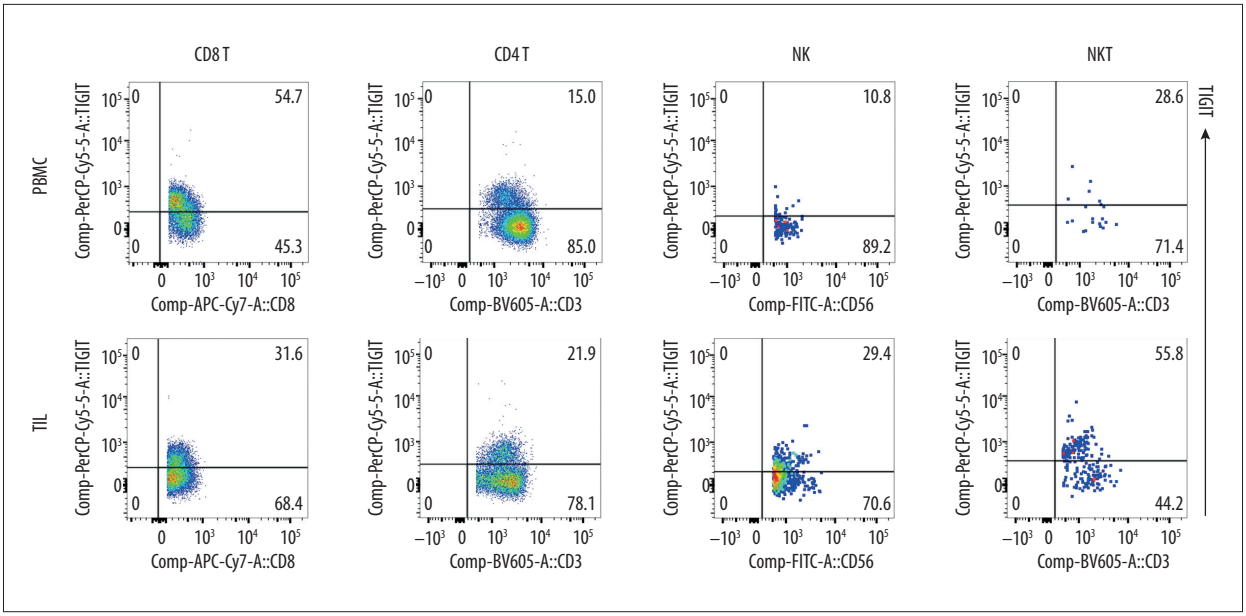

Figure 3. TIGIT expression on lymphocytes. TIGIT expression on TILs and PBMC (CD8⁺T, CD4⁺T, NK, and NKT). TIGIT expression in these cells was significantly higher than PD-1 expression.

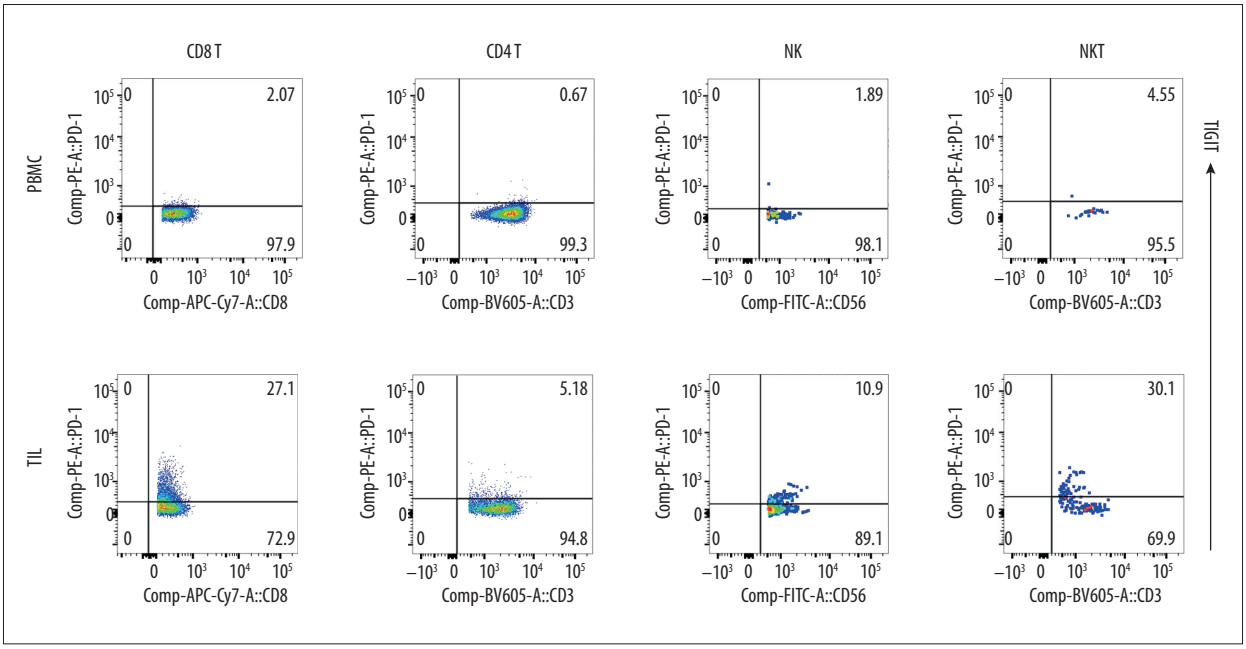

Figure 4. PD-1 expression on lymphocytes. PD-1 expression on TILs and PBMC (CD8⁺T, CD4⁺T, NK, and NKT). PD-1 expression in these cells was significantly lower than TIGIT expression.

in 9 tissues, with a positive rate of 15.0% (9/60). The chi-square test indicated significant differences in the PD-1 positive rate between ccRCC tissues and adjacent normal tissues ($P=0.007<0.05$) (Table 2).

Correlation of PD-1 expression in ccRCC with clinicopathological characteristics

The positive PD-1 expression had no relationship with age, sex, or TNM stage ($P>0.05$), but was closely correlated to tumor diameter and Fuhrman grade ($P<0.05$). The PD-1 positive rate in patients with tumor diameter >4.0 cm (48.5%) was significantly higher than in those with tumor diameter ≤4.0 cm.

Indexed in: [Current Contents/Clinical Medicine] [SCI Expanded] [ISI Alerting System] [ISI Journals Master List] [Index Medicus/MEDLINE] [EMBASE/Excerpta Medica] [Chemical Abstracts/CAS]

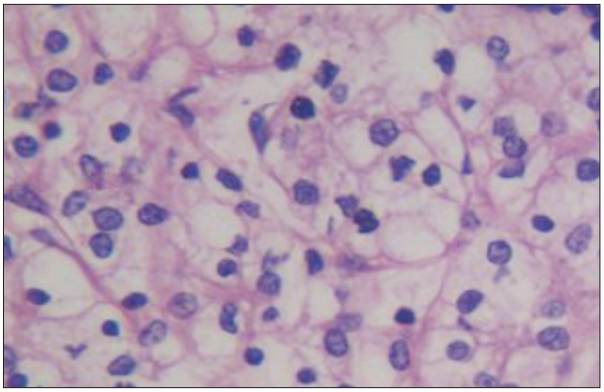

Figure 5. HE staining of ccRCC (×400). The majority of cells showed transparent cytoplasm with clear boundary, the small and round nucleus localizes at the center in most cells, few cells showed atypia, and several cells showed dark nuclear staining with mild atypia. The interstitium was rich in blood vessels and mild fibrous hyperplasia was observed.

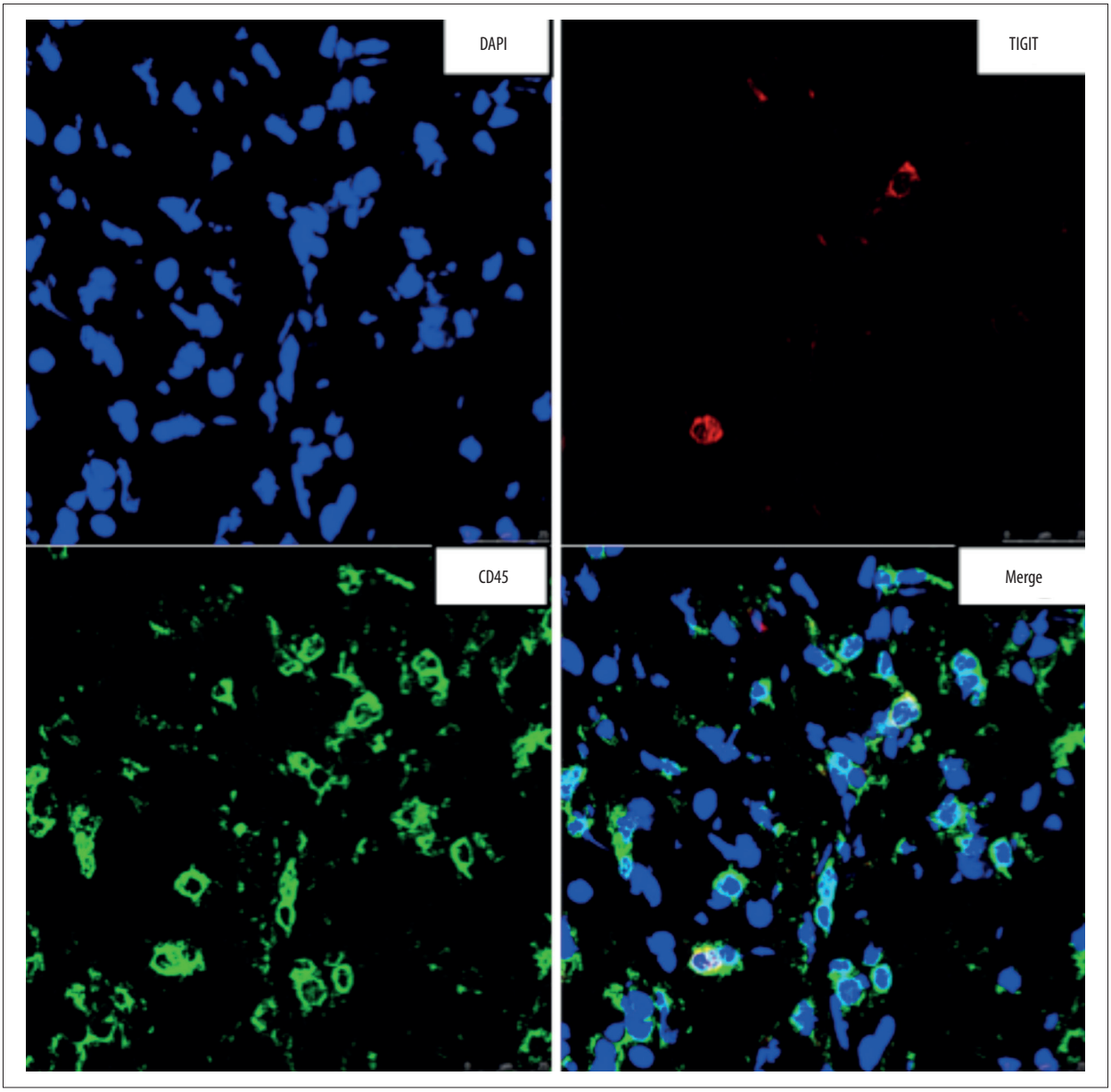

Figure 6. TIGIT expression in ccRCC. TIGIT expression was detectable in ccRCC, and confocal microscopy showed TIGIT expression on CD45-positive cells.

Indexed in: [Current Contents/Clinical Medicine] [SCI Expanded] [ISI Alerting System] [ISI Journals Master List] [Index Medicus/MEDLINE] [EMBASE/Excerpta Medica] [Chemical Abstracts/CAS]

Table 2. PD-1 expression in ccRCC and adjacent normal tissues.

Sites	Positive	Negative	Total	Positive rate (%)
ccRCC	22	38	60	36.7
Adjacent normal tissues	9	51	60	15.0
Total	31	89	120	25.8

χ^2=7.350, P=0.007.

Table 3. Correlation of PD-1 expression in ccRCC with clinicopathological characteristics.

	n	PD-1				Positive rate (%)	P
		–	+	++	+++		
Age (year)							0.428
≤50	26	15	7	4	0	42.3	
>50	34	23	9	1	1	32.4	
Sex							0.282
Male	38	26	9	2	1	31.6	
Female	22	12	7	3	0	45.5	
Tumor diameter (cm)							0.036
≤4.0	27	21	4	2	0	22.2	
>4.0	33	17	10	5	1	48.5	
Fuhrman grade							0.047
Well differentiated	45	32	9	4	0	28.9	
Intermediately differentiated	10	5	1	3	1	50.0	
Poorly differentiated	5	1	1	2	1	80.0	
TNM stage							0.071
Stage I	40	29	8	3	0	27.5	
Stage II	16	8	3	4	1	50.0	
Stage III	4	1	1	1	1	75.0	

Chi-square test with continuity correction: P<0.05.

Moreover, the PD-1-positive rate in patients with highly differentiated ccRCC (28.9%) was significantly lower than in those with poorly differentiated ccRCC (80.0%) according to the Fuhrman grading system (P=0.040<0.05), but a marked difference was not observed between any other 2 groups (P>0.05) (Table 3).

TIGIT expression in ccRCC and adjacent normal tissues

TIGIT was mainly expressed on T cells and NK cells. In 60 ccRCC tissues, TIGIT-positive expression was found in 45 tissues, with a positive rate of 75% (45/60). In 60 adjacent normal tissues, the TIGIT-positive rate was 48.3% (29/60). The chi-square test showed a significant difference in the TIGIT-positive rate between ccRCC tissues and adjacent normal tissues (P=0.003<0.05) (Table 4).

Correlation of TIGIT expression in ccRCC with clinicopathological characteristics

The TIGIT-positive rate had no relationship with age, sex, tumor diameter, Fuhrman grade, or TNM stage (P>0.05) (Table 5).

Correlation between PD-1 and TIGIT in ccRCC

In 60 ccRCC tissues, 18 were positive for both PD-1 and TIGIT and 11 were negative for both PD-1 and TIGIT; 4 tissues were positive for PD-1 but negative for TIGIT; and 27 tissues were negative for PD-1 but positive for TIGIT. Spearman rank correlation analysis showed there was no significant correlation between PD-1 and TIGIT in ccRCC (r=0.120, P=0.362>0.05) (Table 6).

Indexed in: [Current Contents/Clinical Medicine] [SCI Expanded] [ISI Alerting System] [ISI Journals Master List] [Index Medicus/MEDLINE] [EMBASE/Excerpta Medica] [Chemical Abstracts/CAS]

Table 4. TIGIT expression in ccRCC and adjacent normal tissues.

Sites	Positive	Negative	Total	Positive rate (%)
ccRCC	45	15	60	75.0
Adjacent normal tissues	29	31	60	48.3
Total	74	46	120	61.7

χ^2=9.025, P=0.003.

Table 5. Correlation of TIGIT expression in ccRCC with clinicopathological characteristics.

	n	PD-1				Positive rate (%)	P
		–	+	++	+++		
Age (year)							0.367
≤50	26	8	10	6	2	69.2	
>50	34	7	15	7	5	79.4	
Sex							0.757
Male	38	10	10	9	9	73.7	
Female	22	5	7	6	4	77.3	
Tumor diameter (cm)							0.178
≤4.0	27	9	4	10	4	66.7	
>4.0	33	6	12	8	7	81.8	
Fuhrman grade							0.551
Well differentiated	45	13	17	10	5	71.1	
Intermediately differentiated	10	1	1	5	3	90.0	
Poorly differentiated	5	1	1	1	2	80.0	
TNM stage							0.341
Stage I	40	12	11	13	4	70.0	
Stage II	16	3	3	4	6	81.3	
Stage III	4	0	1	1	2	100.0	

Chi-square test with continuity correction: P<0.05.

Table 6. Correlation between PD-1 and TIGIT in ccRCC.

PD-1	TIGIT		Total
	+	–	
+	18	4	22
–	27	11	38
Total	45	15	60

r=0.120, P=0.362.

Correlation of PD-1 expression with distance to ccRCC

The PD-1 expression was related to the distance of adjacent normal tissues to ccRCC (P=0.000<0.05). Paired comparisons showed no significant difference in PD-1 expression between ccRCC and interface tissues, between ccRCC and 0.5-cm tissues, or between interface tissues and 0.5-cm/1.0-cm/2.0-cm tissues (P>0.05). However, a marked difference in PD-1 expression was noted between ccRCC and 1.0-cm tissues (P=0.007<0.05), between ccRCC and 2.0-cm tissues (P=0.000<0.05), between interface tissues and 1.0-cm tissues (P=0.001<0.05), between interface tissues and 2.0-cm tissues (P=0.000<0.05), between 0.5-cm tissues and 1.0-cm tissues (P=0.019<0.05), and between 0.5-cm tissues and 2.0-cm tissues (P=0.000<0.05) (Table 7).

Spearman rank correlation analysis of PD-1 expression with distance of adjacent normal tissues to ccRCC showed that the PD-1 expression was closely related with the distance of adjacent normal tissues to ccRCC: longer distance was associated with lower PD-1 expression and PD-1-positive rate.

Indexed in: [Current Contents/Clinical Medicine] [SCI Expanded] [ISI Alerting System] [ISI Journals Master List] [Index Medicus/MEDLINE] [EMBASE/Excerpta Medica] [Chemical Abstracts/CAS]

Table 7. Correlation of PD-1 and TIGIT expression with distance to ccRCC.

		Level				Positive rate (%)	χ^2	*P* value
		–	1+	2+	3+			
ccRCC	PD-1	38	15	6	1	36.7	17.88	<0.001
	TIGIT	15	18	17	10	75.0		
Interface tissues	PD-1	35	14	10	1	41.7	6.56	0.010
	TIGIT	21	17	14	8	65.0		
0.5-cm tissues	PD-1	40	12	6	2	33.3	4.13	0.042
	TIGIT	29	15	10	6	51.7		
1.0-cm tissues	PD-1	51	8	1	0	15.0	14.11	<0.001
	TIGIT	32	13	10	5	46.7		
2.0-cm tissues	PD-1	57	3	0	0	5.0	9.41	0.002
	TIGIT	45	12	2	1	25.0		

Correlation of TIGIT expression with distance to ccRCC

The TIGIT expression was correlated to the distance to ccRCC (P=0.000<0.05). Paired comparisons showed no significant difference in TIGIT expression between ccRCC and interface tissues, between interface tissues and 0.5-cm tissues, and between 0.5-cm tissues and 1.0-cm tissues (P>0.05). However, marked differences in TIGIT expression were noted between ccRCC and 0.5-cm tissues (P=0.008<0.05), between ccRCC and 1.0-cm tissues (P=0.000<0.05), between ccRCC and 2.0-cm tissues (P=0.000<0.05), between interface tissues and 1.0-cm tissues (P=0.043<0.05), between interface tissues and 2.0-cm tissues (P=0.000<0.05), between 0.5-cm tissues and 2.0-cm tissues (P=0.003<0.05), and between 1.0-cm tissues and 2.0-cm tissues (P=0.013<0.05) (Table 7).

Spearman rank correlation analysis of TIGIT expression with distance of adjacent normal tissues to ccRCC showed that the TIGIT expression had a close relationship with the distance of adjacent normal tissues to ccRCC: a longer distance was associated with lower TIGIT expression and lower TIGIT-positive rate.

In ccRCC, positive PD-1 expression was significantly lower than TIGIT (36.7% *vs.* 75%, P<0.001). In interface tissue, positive PD-1 expression was significantly lower than TIGIT (41.7% *vs.* 65%, P=0.010<0.05). In 0.5-cm tissues, positive PD-1 expression was significantly lower than TIGIT (33.3% *vs.* 51.7%, P=0.042<0.05). In 1.0-cm tissues, positive PD-1 expression was significantly lower than TIGIT (15.0% *vs.* 46.7%, P<0.001). In 2.0-cm tissues, positive PD-1 expression was significantly lower than TIGIT (5% *vs.* 25%, P=0.002<0.05).

Discussion

The occurrence, development, and metastasis of RCC are regulated by multiple genes and involve multiple factors at different levels. With the rapid development of genomics, proteomics, and metabolomics, the gene variations related to tumorigenesis of tubular epithelial cells have been further elucidated and more pathways involved in this process have been identified, which provide evidence for the development of methods for diagnosis and treatment of RCC [13].

In this study, immunofluorescence staining, flow cytometry, and immunohistochemistry were employed to detect the expression of PD-1 and TIGIT in ccRCC and adjacent normal tissues. The correlation of PD-1 and TIGIT expression with clinicopathological characteristics of ccRCC, the correlation between PD-1 and TIGIT, and the correlation of PD-1 and TIGIT expression with distance to ccRCC were further evaluated. Our findings indicate PD-1 and TIGIT expression are closely related to the occurrence, development, and outcome of RCC.

PD-1 pathway activation in cancer may exert negative regulatory effects and can inhibit the immune response to cancer cells, which is an important mechanism underlying immune escape of cancer cells. The poor therapeutic efficacy might be, at least partially, ascribed to the inhibitory pathways, including the PD-1 pathway. Thus, block these inhibitory pathways (such as the PD-1 pathway) may be a good way to reduce the inhibitory immune regulation and indirectly strengthen the anti-tumor immunity. To date, antibodies targeting PD-1 approved by the FDA of USA include nivolumab (Opdivo; US Bristol-Myers Squibb Company; humanized IgG4 monoclonal antibody) and pembmlizumab (Keytmda, Merck USA; humanized IgG4 monoclonal antibody). Topalian et al. [14] published a phase I clinical trial on nivolumab in the New England Journal of Medicine

Indexed in: [Current Contents/Clinical Medicine] [SCI Expanded] [ISI Alerting System] [ISI Journals Master List] [Index Medicus/MEDLINE] [EMBASE/Excerpta Medica] [Chemical Abstracts/CAS]

in 2012, in which 296 patients with different cancers were recruited (including 33 patients with RCC). Patients were intravenously injected with nivolumab, and results showed the objective remission rate (CR+PR) was 27% and the safety was good. Motzer et al. [15] conducted a phase II clinical trial on nivolumab in which 168 patients developing metastatic renal clear cell carcinoma after targeted therapy were recruited. Results showed the objective remission rate was 21%, an additional 41% of patients showed stable disease, 54% of patients with objective remission showed effectiveness longer than 12 months, the safety was favorable, and the incidence of grade 3/4 adverse effects was 11%. Motzer et al. [16] published a phase III clinical trial in the New England Journal of Medicine in which the therapeutic efficacy was compared between nivolumab and everolimus in patients with advanced RCC. In that study, 821 patients with advanced ccRCC were recruited, and results showed the median OS was 25.0 months in the nivolumab group, which was significantly longer than in the everolimus group (19.6 months), the RR of death was 0.73, showing better survival in nivolumab group, and the objective remission rate was 25% and 5% in the nivolumab group and everolimus group, showing a significant difference. This phase III study further confirms anti-PD-1 treatment is effective and safe for patients with advanced RCC. On the basis of findings from phase I, phase II, and phase III studies, the therapeutic efficacy and safety of nivolumab treatment are favorable for RCC patients, but a clear dose-response relationship has not been established. This indicates that the PD-1 pathway is only a tip of the iceberg in the target anti-tumor therapy [17]. Of note, the effectiveness of anti-CTLA-4 and anti-PD-1 treatment is not observed in all types of cancers but is mainly found in those with some solid cancers [18]. In respect to co-expression of other molecules with PD-1/PD-L1 in the tumor microenvironment, it is necessary to investigate the specific mechanisms underlying the immune escape of cancer cells in a specific cancer. The present study focused on TIGIT as a potential target for the RCC treatment.

TIGIT is a new immunomodulatory molecule and has the following characteristics: (1) TIGIT is an immunosuppressive molecule of effector T cells and can antagonize the CD226 mediated costimulatory signals. TIGIT is mainly expressed on activated memory $CD4^+CD45RO^+$ cells, but not on naive $CD4^+CD45RO^-$ T cells [19]. Kuchroo et al. [19] found TIGIT was able to reduce the threshold of T cell activation. Further gene microassay showed activation of TIGIT on T cells could down-regulate the expression of molecules related to TCR/CD28 activation and the cycle progression was then inhibited. This suggests that there is a TIGIT-mediated mechanism in T cells contributing to the negative regulation of immunity. (2) TIGIT is a marker of human Treg cells. Foxp3 is a specific transcription factor related to Treg related cell development and function. It can activate the transcription of immune inhibitory genes such as CTLA-4 and also inhibit the transcription of immune activation genes such as IL-2 and IFN-r. In recent years, studies revealed there is a binding site of Foxp3 in the promoter of the human TIGIT gene [20]. There is evidence showing TIGIT is a marker differentiating nTreg cells and effector T cells activated *in vitro*. (3) TIGIT is a co-inhibitory molecule of NK cells. As in T cells, NK cells also express CD226 and TIGIT, which are 2 molecules that act as co-stimulatory and co-inhibitor signals, respectively, to regulate the activation of NK cells. In addition, CD155/CD226 and CD112/CD226 can provide activation signals, but CD155/TIGIT and CD112/TIGIT provide inhibitory signals. After CD155 stimulates human NK cells, the Tyr225 close to the ITIM motif in the tail of TIGIT in the cytoplasm is phosphorylated and then binds to adapter protein Grb2. Subsequently, SH2 (Src homology 2)-containing inositol phosphatase-1 (SHIP1) is recruited to stop the PI3K and MAPK signaling, resulting in the inhibition of NK cell functions [21]. (4) TIGIT may also affect DCs. CD155 on DCs may serve as a ligand to TIGIT. TIGIT may phosphorylate the intracellular segment of CD155 to activate MAPK Erk pathway, which regulates the cytokine secretion of DCs (increase in IL-10 and reduction in IL-12). After TIGIT-Fc treatment, the ability of DCs to stimulate the proliferation of T cells is compromised [19]. (5) TIGIT may also affect the follicular helper T cells (Tfh). Recent studies indicate that Tfh cells have a high expression of TIGIT but have no CD226 expression, while FDCs show high CD155 expression. TIGIT/CD155 may mediate the adhesion between Tfh cells and FDC. This indicates that the expression of TIG1T/CD226 changes dynamically in the differentiation of Th cells into different cell subsets [22].

Conclusions

Great progress has been achieved in the PD-1/PD-L1 pathway-related target therapy of RCC, and the favorable disease control rate provides new promise for the treatment of advanced RCC. This study for the first time investigated the TIGIT expression in RCC and its relationship with clinicopathological characteristics, Fuhrman grade, and TNM stage of RCC, and this information was compared with that of the PD-1/PD-L1 pathway. We speculate that TIGIT is an important immune binding molecule involved in the immune regulation of cancer and may become a potential target for the ccRCC treatment. In future studies, the influence of TIGIT on the CD8/CD4 ratio, number and proportion of Treg cells, and ratio of MDSC as well as on other immune binding molecules will be investigated, its influence on CTL activity (such as Granzyme B/Perforin, IFN-γ and TNF-α) will be elucidated, as will the role of the TIGIT signaling pathway in the regulation of RCC growth. Moreover, the relationship between differentially expressed genes determined by RNAseq and TIGIT pathway should be further confirmed. These investigations may provide theoretical evidence for the design and screening of targets for pharmacotherapy

Indexed in: [Current Contents/Clinical Medicine] [SCI Expanded] [ISI Alerting System] [ISI Journals Master List] [Index Medicus/MEDLINE] [EMBASE/Excerpta Medica] [Chemical Abstracts/CAS]

of RCC and their clinical application. We also intend to focus the mechanism of the TIGIT signaling pathway in ccRCC immune regulation, including correlation of TIGIT with RNAseq expression of different immune cells, expression of the TIGIT signaling pathway in RCC a mouse model and its anti-tumor effects, and effects of blocking the TIGIT signaling pathway on TILs immune responses in ccRCC.

References:

1. Karumanchi SA, Merchan J, Sukhatme VP: Renal cancer: Molecular mechanisms and newer therapeutic options. Curr Opin Nephrol Hypertens, 2002; 11: 37–42
2. Pal SK, Haas NB: Adjuvant therapy for renal cell carcinoma: Past, present, and future. Oncologist, 2014; 19: 851–59
3. Bhatt JR, Finelli A: Landmarks in the diagnosis and treatment of renal cell carcinoma. Nat Rev Urol, 2014; 11: 517–25
4. Gonzalez J, Cozar JM, Gomez A et al: Nephron-sparing surgery in renal cell carcinoma: Current perspectives on technical issues. Curr Urol Rep, 2015; 16: 6
5. Motzer RJ, Hutson TE, Tomczak P et al: Sunitinib versus interferon alfa in metastatic renal-cell carcinoma. N Engl J Med, 2007; 356: 115–24
6. Luo Y, Chen SS, Bai L et al: Nephron sparing surgery has better oncologic outcomes than extirpative nephrectomy in T1a but Not in T1b or T2 stage renal cell carcinoma. Med Sci Monit, 2017; 23: 3480–88
7. Eggener SE, Yossepowitch O, Pettus JA et al: Renal cell carcinoma recurrence after nephrectomy for localized disease: Predicting survival from time of recurrence. J Clin Oncol, 2006; 24: 3101–6
8. Couzin-Frankel J: Breakthrough of the year 2013. Cancer immunotherapy. Science, 2013; 342: 1432–33
9. Frebel H, Nindl V, Schuepbach RA et al: Programmed death 1 protects from fatal circulatory failure during systemic virus infection of mice. J Exp Med, 2012; 209: 2485–99
10. Topalian SL, Drake CG, Pardoll DM: Targeting the PD-1/B7-H1(PD-L1) pathway to activate anti-tumor immunity. Curr Opin Immunol, 2012; 24: 207–12
11. Stengel KF, Harden-Bowles K, Yu X et al: Structure of TIGIT immunoreceptor bound to poliovirus receptor reveals a cell-cell adhesion and signaling mechanism that requires cis-trans receptor clustering. Proc Natl Acad Sci USA, 2012; 109: 5399–404
12. Blake SJ, Dougall WC, Miles JJ et al: Molecular pathways: Targeting CD96 and TIGIT for cancer immunotherapy. Clin Cancer Res, 2016; 22: 5183–88
13. Callea M, Albiges L, Gupta M et al: Differential expression of PD-L1 between primary and metastatic sites in clear-cell renal cell carcinoma. Cancer Immunol Res, 2015; 3: 1158–64
14. Topalian SL, Hodi FS, Brahmer JR et al: Safety, activity, and immune correlates of anti-PD-1 antibody in cancer. N Engl J Med, 2012; 366: 2443–54
15. Motzer RJ, Rini BI, McDermott DF et al: Nivolumab for metastatic renal cell carcinoma: Results of a randomized phase II trial. J Clin Oncol, 2015; 33: 1430–37
16. Motzer RJ, Escudier B, McDermott DF et al: Nivolumab versus everolimus in advanced renal-cell carcinoma. N Engl J Med, 2015; 373: 1803–13
17. Balar AV, Weber JS: PD-1 and PD-L1 antibodies in cancer: Current status and future directions. Cancer Immunol Immunother, 2017; 66: 551–64
18. Hoos A, Ibrahim R, Korman A et al: Development of ipilimumab: Contribution to a new paradigm for cancer immunotherapy. Semin Oncol, 2010; 37: 533–46
19. Lozano E, Dominguez-Villar M, Kuchroo V, Hafler DA: The TIGIT/CD226 axis regulates human T cell function. J Immunol, 2012; 188: 3869–75
20. Levin SD, Taft DW, Brandt CS et al: Vstm3 is a member of the CD28 family and an important modulator of T-cell function. Eur J Immunol, 2011; 41: 902–15
21. Liu S, Zhang H, Li M et al: Recruitment of Grb2 and SHIP1 by the ITT-like motif of TIGIT suppresses granule polarization and cytotoxicity of NK cells. Cell Death Differ, 2013; 20: 456–64
22. Boles KS, Vermi W, Facchetti F et al: A novel molecular interaction for the adhesion of follicular CD4 T cells to follicular DC. Eur J Immunol, 2009; 39: 695–703

Indexed in: [Current Contents/Clinical Medicine] [SCI Expanded] [ISI Alerting System] [ISI Journals Master List] [Index Medicus/MEDLINE] [EMBASE/Excerpta Medica] [Chemical Abstracts/CAS]